Dopamine modulates synaptic plasticity in dendrites of rat and human dentate granule cells

Trevor J. Hamilton[a,b], B. Matthew Wheatley[c], D. Barry Sinclair[d], Madeline Bachmann[a], Matthew E. Larkum[e], and William F. Colmers[a,b,1]

[a]Department of Pharmacology and [b]Centre for Neuroscience, University of Alberta, Edmonton, AB, Canada T6G 2H7; [c]Division of Neurosurgery, University of Alberta, Edmonton, AB, Canada T6G 2B7; [d]Department of Pediatrics, University of Alberta, Edmonton, AB, Canada T6G 2J3; and [e]Department of Physiology, University of Berne, CH-3012 Berne, Switzerland

Edited by Floyd Bloom, The Scripps Research Institute, La Jolla, CA, and approved September 8, 2010 (received for review August 5, 2010)

The mechanisms underlying memory formation in the hippocampal network remain a major unanswered aspect of neuroscience. Although high-frequency activity appears essential for plasticity, salience for memory formation is also provided by activity in ventral tegmental area (VTA) dopamine projections. Here, we report that activation of dopamine D1 receptors in dentate granule cells (DGCs) can preferentially increase dendritic excitability to both high-frequency afferent activity and high-frequency trains of back-propagating action potentials. Using whole-cell patch clamp recordings, calcium imaging, and neuropeptide Y to inhibit postsynaptic calcium influx, we found that activation of dendritic voltage-dependent calcium channels (VDCCs) is essential for dopamine-induced long-term potentiation (LTP), both in rat and human dentate gyrus (DG). Moreover, we demonstrate previously unreported spike-timing–dependent plasticity in the human hippocampus. These results suggest that when dopamine is released in the dentate gyrus with concurrent high-frequency activity there is an increased probability that synapses will be strengthened and reward-associated spatial memories will be formed.

dentate gyrus | long-term potentiation | neuropeptide Y | dopamine D1 receptor | dendritic excitability

As an animal explores a specific location, place cells in the dentate gyrus (DG) of the hippocampus fire bursts of action potentials (APs) (1) that can result in the formation of a new, long-term contextual memory (2). This is part of the "pattern separation" mechanism, whereby only a small population of dentate granule cells (DGCs) become very active and pass on the incoming cortical input to be later represented or "completed," in the downstream CA3 network (3). Memory formation related to a specific place can be enhanced by an associated salience, such as reward (4). Recent work suggests that disruption of mesocorticolimbic dopamine responses blocks conditioned place preference (CPP), a reward-driven form of spatial memory (5, 6). Furthermore, nicotine-induced CPP requires dopamine D1 receptor (D1R) activation in the DG (7). The medial perforant pathway (MPP) carries spatial information to the middle third of the molecular layer (8). In DGCs, D1Rs are concentrated throughout the dendritic tree (9). This suggests that bursting activity in DGCs, coincident with local dopamine release, may enhance formation of salient memories, but a mechanism remains unknown.

One potential mechanism mediating plasticity is the coincidence of backpropagating dendritic APs with appropriately timed synaptic input (10); this mechanism requires postsynaptic Ca^{2+} influx (11). Ca^{2+} channels have been implicated in nonlinear, frequency-dependent responses in dendrites (12) and D1Rs can potentiate dendritic excitability in hippocampal area CA1 (13). Because the molecular layer of the DG is innervated by dopaminergic terminals from the ventral tegmental area (VTA) (14) we examined the possibility that interactions at the level of DGC dendrites between firing frequency, dendritic Ca^{2+} responses, and D1Rs, may mediate plasticity in medial perforant path synaptic inputs.

Results

To investigate the impact of high-frequency input to the DG, we stimulated the medial perforant path with trains of four subthreshold excitatory postsynaptic potentials (EPSPs) while recording from DGCs with an intracellular whole-cell electrode (Fig. 1*A*). As we increased the frequency of trains from 20 to 150 Hz (10-Hz increments) we routinely observed that the synaptic response became nonlinear at upper frequencies (Fig. 1*B*). We hypothesized that this was due to an increased influx of postsynaptic Ca^{2+} through voltage-dependent Ca^{2+} channels (VDCCs) and/or NMDA receptors in the soma and/or dendrites of the DGCs. To test this, we applied neuropeptide Y (NPY), which is known to act only postsynaptically in the DG and inhibit N-type VDCCs (15, 16). NPY fibers from hilar interneurons form a dense projection to the outer two-thirds of the DG molecular layer, where they innervate dendrites of DGCs that densely express NPY1 receptors (17). However, the influence of this NPY system on dentate activity is unknown (18). In the presence of picrotoxin and enhanced Mg^{2+}, application of NPY (1 μM) significantly decreased the nonlinear response (Fig. 1*C*). Conversely, the D1-receptor agonist SKF 81297 (10 μM) enhanced the synaptic nonlinearity in these cells (Fig. 1*D*). These results indicate that this nonlinear response to high-frequency input is subject to neuromodulation.

To examine the consequences of high-frequency postsynaptic activity in DGC dendrites, we emulated bursting behavior with trains of four somatic APs (40–150 Hz) in DGCs filled via the patch pipette with the Ca^{2+} indicator dye, Oregon Green BAPTA-1 (OGB-1) (Fig. 1*E*). We compared five regions of interest (ROIs) along a DGC dendrite (Fig. 1*F*) and normalized the Ca^{2+} transients (ΔF/F measurement) to the lowest frequency (40 Hz) train of APs for each ROI. In control artificial cerebrospinal fluid (ACSF), normalized Ca^{2+} transients did not increase with AP frequency in the most proximal dendritic compartments, but more distal ROIs did exhibit frequency-dependent increases. The most distal ROI showed the largest relative increase in Ca^{2+} transient with frequency (Fig. 1*G*). By contrast, in the same DGCs, there was no significant increase in the time-voltage integral of somatic depolarization after the final AP in the train (Fig. S1). This index has been shown to be sensitive to regenerative dendritic activity (12, 19). These results are consistent with a frequency-dependent regenerative event that occurs at the DGC distal dendrite and normally does not conduct to the soma.

We hypothesized that the efficiency of coupling between the distal dendrite and the soma might be reduced by conductances from ongoing dendritic synaptic input (20). However, after treat-

Author contributions: T.J.H., M.E.L., and W.F.C. designed research; T.J.H., B.M.W., D.B.S., and M.B. performed research; B.M.W. and D.B.S. performed neurosurgery on epileptic patients; T.J.H. analyzed data; and T.J.H., M.E.L., and W.F.C. wrote the paper.

The authors declare no conflict of interest.

This article is a PNAS Direct Submission.

[1]To whom correspondence should be addressed. E-mail: william.colmers@ualberta.ca.

This article contains supporting information online at www.pnas.org/lookup/suppl/doi:10.1073/pnas.1011558107/-/DCSupplemental.

NEUROSCIENCE

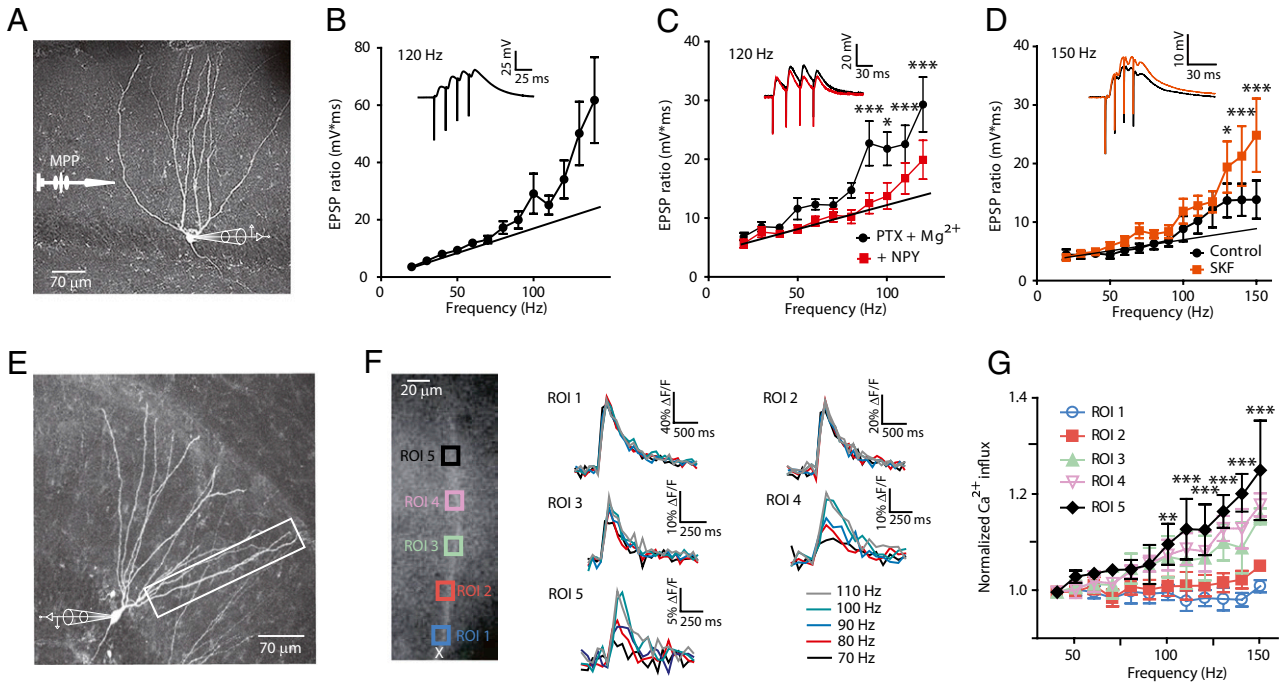

Fig. 1. Frequency-dependent dendritic responses observed in DGCs. (*A*) A neurobiotin-filled DGC with representative whole-cell recording electrode and bipolar stimulation electrode in the MPP. (*B*) Normalized responses to synaptic trains of four EPSPs from 20–150 Hz (10-Hz increments). The time-voltage integral of the entire synaptic train was divided by the time-voltage integral of the first EPSP in the train to give the EPSP ratio (solid black circles) ($n = 10$). (*Inset*) Sample trace at 120 Hz. (*C*) Synaptic responses to higher frequency stimulus trains are sensitive to NPY action. Responses in PTX (100 μM) + elevated Mg^{2+} (to 5 mM) alone are shown in solid black circles and responses in the additional presence of NPY (1 μM) are shown in solid red squares (***$P < 0.001$, *$P < 0.05$; $n = 9$). (*Inset*) Sample traces at 120 Hz. (*D*) Dopamine D1R agonist, SKF 81297 (10 μM) was applied via the bath in control ACSF and trains of EPSPs were evoked as above (***$P < 0.001$, *$P < 0.05$; $n = 6$). (*Inset*) Sample traces at 150 Hz. (*E*) Neurobiotin-filled DGC with representative whole-cell recording and rectangular area of Ca^{2+} imaging. (*F*, *Left*) Square regions of interest (ROIs) used for Ca^{2+} imaging experiments. X is 44 μM from the cell body. (*Right*) Trains of somatic APs induced Ca^{2+} influx measured as $\Delta F/F$ at five ROIs. Distal ROIs 4 and 5 showed sensitivity to higher frequencies, whereas proximal ROIs 1 and 2 did not. (*G*) Ca^{2+} influx was normalized to 40-Hz measurements and compared with frequencies up to 150 Hz (difference between ROIs 1 and 5 (***$P < 0.001$, **$P < 0.01$, $P < 0.05$; $n = 3$). Symbol colors correspond to ROIs in *F*.

ment with picrotoxin (100 μM), APV (50 μM), kynurenic acid (1 mM), and elevated Mg^{2+} (to 5 mM) to block ionotropic GABA and glutamate receptors, respectively, the distal regenerative event still had little or no influence on integration at the soma (Fig. S1). Because A- and D-type K^+ channels regulate dendritic excitability in hippocampal CA1 and neocortical neurons (21–23), we added a modest concentration of the A- and D-type K^+ channel blocker, 4-aminopyridine (4-AP; 100 μM), in addition to the synaptic blockers above ("4-AP solution"). Under these conditions, trains of bAPs above a "critical frequency" (CF) (ref. 12; *Materials and Methods*) that evoked supralinear Ca^{2+} transients distant (>175 μm) from the soma as before, now also coincided with the appearance of a large somatic after-depolarization (ADP) (Fig. 2*A*). The CFs evident both from distal dendritic Ca^{2+} and somatic ADP responses were virtually identical (dendrite: 121 ± 8 Hz; soma: 128 ± 9 Hz; $n = 10$; $P < 0.09$) and were strongly correlated in the dendrites and somata of individual neurons (Fig. 2*B*; $r^2 = 0.8258$; $P < 0.0001$). Thus, in the presence of the 4-AP solution, trains of bAPs at supracritical frequencies induce a distal dendritic Ca^{2+} influx that is tightly related to a somatic ADP, in the absence of NMDA receptor activation (Fig. S1). This suggests that somatodendritic coupling is normally maintained at a relatively low level in DGCs by a subset of strongly 4-AP–sensitive K^+ channels in the dendrites (Table S1).

To determine whether VDCCs mediate the depolarizing potential underlying the CF (12), we applied the nonselective VDCC blocker, Cd^{2+}, via the bath. At 50 μM, Cd^{2+} completely blocked the increase in ADP that was unmasked by 4-AP (Fig. S2). The selective VDCC blockers, nifedipine (5 μM), ω-conotoxin GVIA (5 μM), and Ni^{2+} (50 μM), each partially inhibited the ADP and increased the CF, indicating that L-, N-, and T-type VDCCs, respectively, all contribute to the ADP seen in the presence of 4-AP (Fig. S2). We hypothesized that Ca^{2+} influx through distal dendritic VDCCs mediates the CF voltage response. To address this hypothesis, we unmasked somatic ADPs with the 4-AP solution as above and then blocked Ca^{2+} influx with localized application of Cd^{2+} to the soma, the proximal, or the distal dendrites (50–100 μm and 120–250 μm from the soma, respectively). ACSF containing Cd^{2+} (100 μM) and Alexa 594 (500 nM) was pressure-ejected under visual guidance from an applicator micropipette onto DGCs also loaded with Alexa 594 (5 μM; Fig. 2*C*). In some DGCs we first applied Cd^{2+} at the soma, then at the proximal dendrites, and finally at a distal dendritic locus. In others we reversed the order of application. Cd^{2+} only inhibited the ADP and altered the CF when it was applied distally (Fig. 2*D*), where it resulted in a mean CF change of 19 ± 4 Hz (Fig. 2*E*; *$P < 0.005$). This result suggests that distal dendritic VDCCs underlie the local generation of frequency-dependent, regenerative responses. In the presence of 4-AP, these appear sufficient to propagate into the soma, resulting in increased excitability.

Because dopamine fibers from the VTA carry reward-based information (4) to the DG (24), and because the entire DGC dendrite bears the D1Rs (9) essential to CPP (7), we tested the hypothesis that D1R activation would unmask and/or potentiate ADPs in rat DGCs. In some DGCs tested in control ACSF alone, the D1R agonist SKF 81297 (SKF) (10 μM) increased the integral of the ADP and unmasked a clear CF with a mean of 110 ± 13 Hz ($n = 5$; Fig. 3*A*); this increase was subsequently inhibited by application of Cd^{2+} and Ni^{2+} in all DGCs tested (Fig. 3*A*). In other DGCs, SKF significantly increased the ADP amplitude across all frequencies, but did not cause a clear CF ($n = 9$). Figure 3 *B* and *C* illustrates these two distinct responses to SKF. SKF effects were antagonized by the D1R antagonist SCH 23390 (Fig. S3).

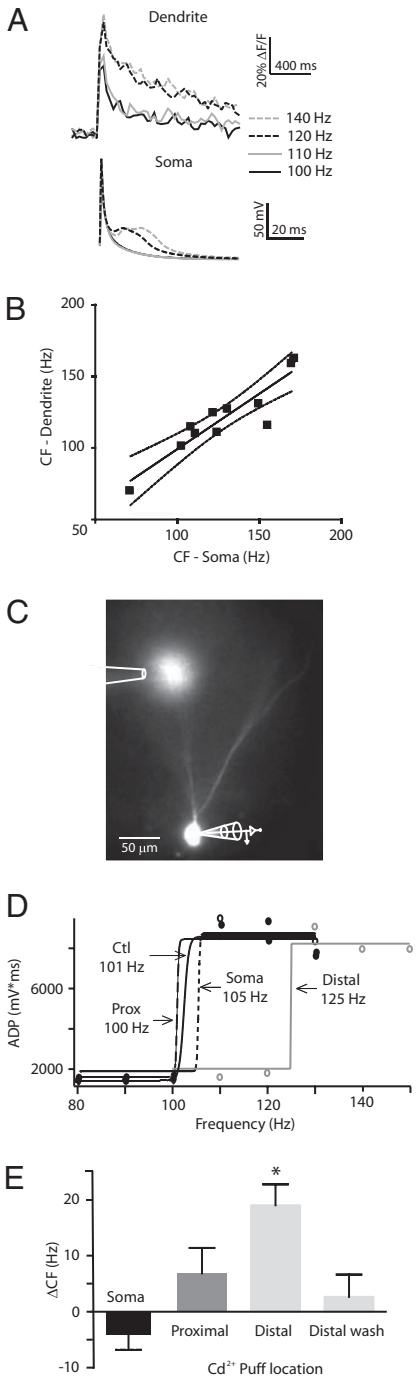

Fig. 2. 4-AP unmasks Ca^{2+}-dependent critical frequencies and after-depolarizations. (*A*) In the presence of 4-AP (100 μM) and synaptic blockers (PTX, 100 μM; APV, 50 μM; kynurenic acid, 100 μM; and Mg^{2+}, to 5 mM) distal dendritic Ca^{2+} transients (*Above*) recorded at 200 μm from the soma become supracritical at the same frequencies as the somatic ADP (120 Hz; *Below*). (*B*) Correlation of dendritic and somatic CFs recorded simultaneously (as in *A*) in individual DGCs ($r^2 = 0.8258$; $P < 0.0001$; $n = 12$). (*C*) Cd^{2+} (100 μM) was applied locally from a puffer pipette also containing Alexa 594 (500 nM). Experiments were performed in the presence of the 4-AP solution in DGCs filled with Alexa 594 (1 μM). (*D*) Plot of ADP time-voltage integral in a single DGC as a function of frequency. The sigmoidal fit was used to determine the CF (shown) for responses in 4-AP (Ctl), and with subsequent local applications of Cd^{2+} to the soma, proximal (Prox) and distal dendrites. In this DGC, distal and somatic application of Cd^{2+} produced a 24-Hz and 4-Hz rightward shift, respectively; however, the shift caused by soma application was not significant across DGCs. (*E*) Change in CF after local Cd^{2+} application to the soma (−5 ± 2 Hz; $n = 9$) proximal dendrite (7 ± 5 Hz; $n = 5$), distal dendrite (19 ± 4 Hz; $n = 8$), and during washout after distal application (3 ± 4 Hz; $n = 7$; $^*P < 0.05$).

As the effects of SKF were very similar to those of 4-AP, we tested whether the effects of 4-AP and SKF on CFs were additive. In the presence of a low (10 μM) concentration of 4-AP (plus the synaptic blockers as above), some DGCs never exhibited a CF or an increase in the ADP, but the addition of 10 μM SKF unmasked a robust CF, which reversed upon washout of SKF (Fig. S3). Furthermore, a local application of 4-AP (100 μM) to distal dendrites in the presence of SKF (10 μM) that did not evoke a CF still resulted in an increase in the ADP and the appearance of a CF that reversed upon washout of 4-AP (Fig. S3). In neurons in which the higher (100 μM) 4-AP solution unmasked a clear CF and increase in ADP, addition of SKF reversibly increased the magnitude of the ADP and decreased the CF (Fig. 3*D*), consistent with an enhancement of dendritic Ca^{2+} influx. To further test the relationship between D1R and VDCC activation we applied ω-conotoxin GVIA, which antagonized the SKF-induced CF (Fig. S3). Finally, to determine whether the actions of D1R agonists and 4-AP involved a final common pathway, we applied a high (300 μM) concentration of 4-AP and found that SKF no longer had an additive effect on the ADP (Fig. S3). These results suggest that during bursts of DGC firing, D1R activation might result in an inhibition of distal dendritic 4-AP–sensitive K^+ channels (25), an increased activation of N-type and possibly other types of VDCCs, or act via both of these mechanisms.

NPY is known to have only postsynaptic effects on DGCs, specifically the inhibition of N-type VDCCs (15, 16). In contrast to the D1R effects above, agonists for the NPY Y1 receptor (Y1R), but for neither Y2 nor Y5 receptors, reduced the ADP and increased the CF (Fig. S4). After full washout of SKF in four responsive DGCs, application of NPY resulted in a decreased ADP and increased CF (Fig. 3*E*). Furthermore, focal application of NPY (3 μM) to distal dendrites resulted in CF increases and ADP inhibition (Fig. S4). Therefore, neuromodulators can shift dendritic Ca^{2+} activity in both directions in the same DGC (Fig. 3 *E* and *F*).

To determine whether activation of adenylate cyclase by D1Rs could mediate the effect of SKF (4), in a separate group of DGCs we applied the membrane-permeant cAMP analog, dibutyrl-cAMP (db-cAMP; 10 μM) in the presence of the 100 μM 4-AP solution. This resulted in a CF reduction not significantly different from that seen with SKF (Fig. 3*E*; −23 ± 6 Hz, $n = 6$, $P > 0.9$). Finally, to test whether the D1R-mediated decrease in CF could itself be modulated by a local neuromodulator, in neurons in which 10 μM 4-AP alone had no effect, we unmasked a CF with the addition of SKF (10 μM), then added NPY (1 μM) with SKF present. Activation of the Y1R sharply reduced the D1 agonist-induced ADP magnitude at the CF and 10 Hz above it (Fig. 3*F*). These results are consistent with DGC activity-dependent dendritic Ca^{2+} responses being enhanced by dopamine but suppressed by NPY.

The plasticity of excitatory synaptic responses has been linked with changes in dendritic excitability (10, 11, 26). Previous studies of long-term potentiation (LTP) in immature DGCs showed that synaptic inputs can be potentiated after one-to-one pairings of brief trains of EPSPs with APs, repeated at theta frequencies. This LTP is attributed to the enhancement of postsynaptic Ca^{2+} influx caused by these pairings (11, 27). We therefore postulated that enhancement of dendritic Ca^{2+} influx via D1 receptors would facilitate synaptic plasticity in DGCs.

As D1R activation typically increased the responsiveness to a 100-Hz train of bAPs, we tested whether a D1R agonist could permit LTP induction in DGCs with a theta-burst pairing (TBP) protocol (*Materials and Methods*; Fig. 4 *A* and *B*) at an intensity that alone never induced LTP. Synaptic inputs were stimulated focally via a bipolar electrode placed in the MPP, which conveys mainly spatial information and which innervates the middle DGC dendritic segment that normally does not permit the forward propagation of distal Ca^{2+} electrogenesis (Fig. 4*A*; ref. 7).

We studied young DGCs that comprise the innermost granule cell layer (GCL) (IR: 523 ± 52 MΩ; $n = 7$) because of their relatively elevated excitability and lower CFs (Fig. S5). Under control conditions (i.e., in the absence of 4-AP or any synaptic blockers) we observed a small, but not significant, depression in

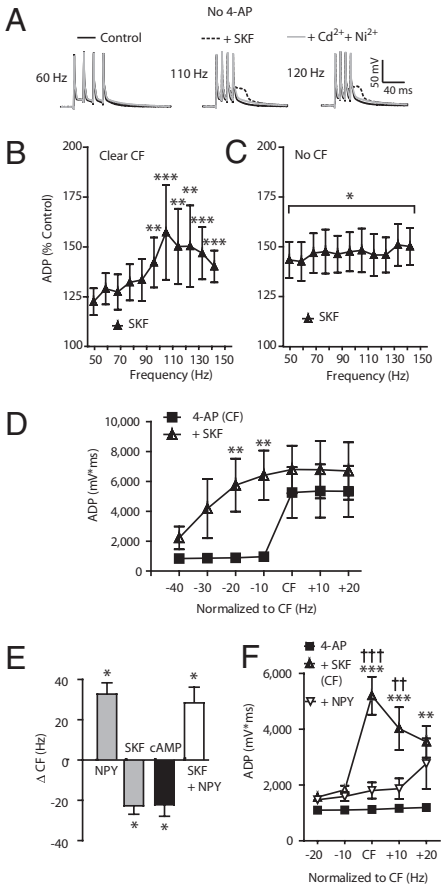

Fig. 3. D1 agonist increases excitability of DGC dendrites. Data in *A–C* were recorded in the absence of 4-AP. (*A*) Sample traces at 60, 110, and 120 Hz shown superimposed in control, in the presence of the D1R agonist SKF 81297 (10 μM) and with Cd^{2+} and Ni^{2+} also added (each 50 μM). SKF application produced two distinct effects: (*B*) Unmasking of a clear CF in some DGCs (mean CF: 110 ± 13 Hz; $^{**}P < 0.01$, $^{***}P < 0.001$; 50 Hz vs. all frequencies; $n = 5$). (*C*) In other DGCs, a significant increase in ADP was seen with SKF across all frequencies (compared with control, $^{*}P < 0.05$), but with no clear CF emerging (no significant differences across all frequencies; $n = 9$). (*D*) In 4-AP (100 μM), SKF increased the ADP and shifted the CF leftward (4-AP vs. SKF, $^{**}P < 0.01$; $n = 6$). (*E*) In 4-AP (100 μM), SKF reversibly decreased the CF by 23 ± 4 Hz ($n = 10$). After a washout of SKF, subsequent NPY application increased the CF by 32 ± 6 Hz ($n = 3$). In other DGCs, the membrane-permeant cAMP analog, dibutyrl-cAMP (10 μM) decreased the CF (23 ± 6 Hz; $n = 6$). Coapplication of SKF and NPY resulted an increase of the CF (mean: 28 ± 7 Hz; $n = 4$) in yet other DGCs. (*F*) In DGCs with no CF in low 4-AP (10 μM), SKF unmasked a CF and increased the ADP integral. Still in the presence of SKF and low 4-AP, NPY inhibited the ADP at and above the CF ($n = 8$; *between 4-AP and SKF; †between SKF and SKF + NPY, ** and $^{\dagger\dagger}P < 0.01$, $^{***}P < 0.001$).

the test response at 1 min after the TBP (75 ± 10% of control; $n = 7$) that returned to control values 10 min later (110 ± 13% of control; $n = 7$). Following the addition of SKF, a repetition of the identical TBP (TBP_2) resulted in a significantly larger ADP during the TBP_2 protocol (Fig. 4*C*), consistent with our previous findings (Fig. 3). Ten minutes after TBP_2, we observed a robust enhancement of the EPSP amplitude in all DGCs tested (Fig. 4*D*; 162 ± 19% of control; $n = 7$). EPSP amplitude remained stably elevated at least 30 min later (142 ± 18% of control; Fig. 4*E*; $P < 0.05$; $n = 7$). By contrast, LTP could be induced neither by repeated TBP protocols nor by application of the dopamine agonist alone (Fig. S6). We next tested whether blockade of postsynaptic VDCCs with NPY (15) could inhibit dopamine-mediated LTP induction. The TBP protocol after application of NPY and SKF via the bath resulted in no change in EPSP amplitude (Fig. S6). Following washout of both compounds, we administered a second TBP in the presence of the D1 agonist only. This resulted in robust LTP (Fig. S6). Finally, focal application of NPY (3 μM) to the distal dendrites (>150 μm from soma) suppressed LTP in the presence of SKF; induction of LTP was again enabled when TBP was applied with SKF again present 10 min after NPY application ceased (Fig. 4*F*). Therefore, D1 receptor-mediated LTP induction in DGCs requires the untrammeled participation of dendritic VDCCs.

In parallel experiments, we performed whole-cell recordings from human DGCs in slices prepared from hippocampal biopsy specimens removed en bloc from patients with medically intractable, temporal lobe epilepsy. The average resting membrane potential (RMP) of human DGCs was −68.5 ± 1.2 mV ($n = 19$), significantly more depolarized than rat DGCs (Table S2), but similar to earlier data from human DGCs (28). As in rat, human DGCs exhibited no significant somatic ADPs in control saline, and the application of 4-AP unmasked robust ADPs (Fig. S7). Aside from the resting potential, properties of human DGCs were qualitatively and quantitatively similar to those of the rat. Specifically, the CF recorded in the presence of 100 μM 4-AP in human DGCs (111 ± 5 Hz; $n = 19$) was not different from the CF of DGCs from any region of the GCL in male or female rats (Table S2). Cd^{2+} (50 μM) also completely abolished the ADP in all human neurons tested (4 of 4; Fig. S7). As in rat, NPY also inhibited the ADP and increased the CF in human DGCs in the presence of 100 μM 4-AP (Fig. S7). Finally, to test the hypothesis that this D1R response could also affect synaptic plasticity in human DGC, we performed TBP experiments on human DGCs in the absence and presence of the D1R agonist, also focally stimulating the MPP. Subthreshold theta-burst pairing was without any long-term effect, but the same protocol repeated in the same cells in the presence of 10 μM SKF, resulted in a significant and sustained LTP in five human DGCs from one male and one female patient (Fig. 4*G*).

Discussion

Dentate granule cells are considered the "gatekeepers" of the hippocampal formation (29, 30). Here we report that DGCs both from rats and from human epilepsy patients have the capacity to express frequency-dependent, backpropagation-activated Ca^{2+} responses, which are normally repressed by dendritic K^+ currents, but can be unmasked by low-to-moderate concentrations of 4-AP. Under physiological conditions, this dendritic Ca^{2+} electrogenesis serves to amplify high-frequency synaptic inputs, and it can be modulated in opposite directions by receptors for NPY and dopamine. In rat DGCs, several types of VDCCs contribute to dendritic Ca^{2+} electrogenesis. Finally, dopamine and potentially other neuromodulators that elevate cAMP (31, 32) can predispose individual rat and human DGCs to the induction of LTP.

Modulation of dendritic excitability is a key aspect of synaptic integration (33). Here we have shown that NPY, by inhibiting distal Ca^{2+} influx via Y1Rs, can affect dendritic electrogenesis in DGCs at both low and high levels of somatodendritic coupling. This is the candidate mechanism for the blockade of dopamine-induced LTP by NPY. Because many interneurons in the hilus express NPY (34), elevated mossy fiber activity is likely in turn to result in enhanced NPY release. Thus, NPY release in the dentate molecular layer would be expected to exert a negative feedback on DGC dendritic excitability, which in turn can profoundly suppress synaptic plasticity.

The VTA dopamine fibers are unique among biogenic amines innervating the hippocampus in that they participate in a reward-detection system that promotes LTP and learning (4, 35, 36). During exploratory behaviors, when gamma-frequency activity occurs in the DG and DGCs fire at high rates (1, 3, 37–39), the reward salience of an external stimulus is signaled by release of dopamine from VTA projections to the molecular layer of the DG (40). Consistent with these observations, in mice where NMDA receptors have been genetically ablated in mesolimbic dopamine neurons, the CPP response to rewards of cocaine or food is impaired (5, 6), suggesting a loss of reward-primed spatial memory

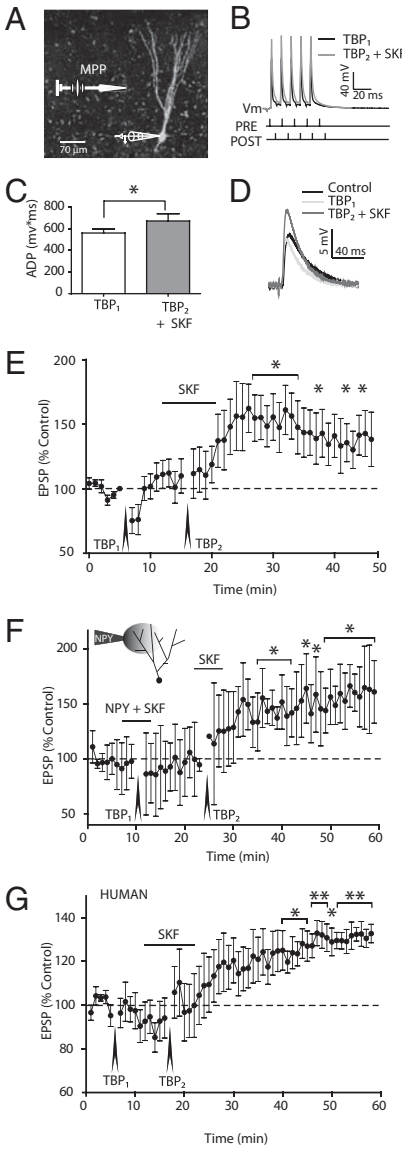

Fig. 4. D1 agonist alters the threshold for LTP induction in rat and human DGCs. (*A*) A neurobiotin-filled human DGC with representative whole-cell recording and extracellular MPP stimulation. (*B*) Sample trace recorded during the theta-burst pairing protocol (TBP_1). The ADP is increased slightly after a subsequent theta-burst pairing (TBP_2) in the presence of bath applied D1 agonist (SKF 81297; 10 μM) in the same DGC (superimposed gray trace). (*C*) The ADP integral was calculated from the onset of the fifth action potential until return to resting potential. Each pair represents a single DGC that exhibited LTP after TBP_2 + SKF (*$P < 0.05$; $n = 7$). (*D*) Sample EPSP traces before (control), after TBP_1, and after TBP_2 + SKF from the same DGC. (*E*) TBP at 100 Hz did not evoke LTP under control conditions (TBP_1). However, with the application of SKF (10 μM) a second TBP (TBP_2) resulted in a long-lasting potentiation (*$P < 0.05$; $n = 7$). (*F*) NPY (3 μM) applied via a focal pipette containing Alexa 594 (300 nM) to the distal dendrites together with bath application of SKF (10 μM) for 4 min before TBP_1 did not change EPSP amplitude 15 min after TBP_1. After washout, SKF (10 μM) was applied alone. Under these conditions, TBP_2 induced LTP (*$P < 0.05$; $n = 4$). (*G*) SKF significantly induces LTP in human DGCs from 350-μm thick hippocampal slices with otherwise the same protocol as in *E* (*$P < 0.05$, **$P < 0.01$; $n = 5$).

formation. Our results indicate that activation of D1Rs on DGCs can increase the magnitude of the ADP and alter tuning to lower frequencies, all of which would promote activity-dependent elevations in dendritic $[Ca^{2+}]_i$ and thus, potentially, synaptic plasticity.

Little is known about the downstream actions of dopamine receptors in the DG (24); however, in pyramidal neurons of hippocampal area CA1, dopamine reportedly modulates dendritic excitability by suppression of dendritic 4-AP–sensitive K^+ channels via protein kinase A (PKA) or protein kinase C (PKC) (25) pathways. D1/D5 receptor activation can also increase excitability via the above mechanism (13). In some DGCs here, D1R activation alone unmasked a CF (Fig. 3 *A* and *B*), comparable to the effect of 4-AP (100 μM). Whereas the D1 agonist was still able to induce a significant CF shift in the presence of 4-AP, this effect saturated with 300 μM 4-AP present (Fig. S3 *G* and *H*). The observed actions of dopamine could thus result from: (*i*) a reduction in 4-AP–sensitive K^+ currents that cause an enhanced somatodendritic coupling; (*ii*) the enhancement of Ca^{2+} electrogenesis by phosphorylation of VDCCs, either directly or via activation of a protein kinase; and (*iii*) a combination of both of the above actions. The mechanism of D1R action remains unclear despite a number of approaches to address it here. Activation of D1Rs was sufficient to permit induction of robust LTP by the otherwise subthreshold TBP stimuli used here, consistent with reports of dopamine-mediated LTP induction in CA1 and prefrontal cortex layer 5 pyramidal cells (41–43). Overall, the results suggest that dopamine, acting at D1Rs, can act as a reward signal that increases dendritic excitability in DGCs and could thereby escort important sensory-based information past the inhibitory "gate" of the DG.

In this study, we focused on the MPP, which innervates the middle DGC dendritic segment, because of its acknowledged role in mediating spatial information (7, 8). Thus, the TBP protocol here was designed to mimic the physiological activation of a place cell (1–3) and the theta oscillations from the entorhinal cortex that occur during exploratory behavior (2, 3). Although we did not examine the LPP here, because D1Rs are distributed uniformly along the dendritic tree of DGCs (9), and VTA dopamine fibers broadly innervate the dentate molecular layer, we anticipate that a similar mechanism could well also facilitate plasticity in the LPP, although this remains to be tested.

In slices of human epileptic hippocampus, D1R receptor activation paired with the TBP protocol can also permit induction of LTP, as in the rat. A previous study using extracellular recordings in human hippocampal slices has shown that LTP in the DG can be induced by either a high-frequency theta stimulus protocol or by increasing intracellular cAMP and that these two methods of induction share a common mechanism (44). Our results using intracellular recordings in human DG suggest that, as in the rat, a cAMP-mediated mechanism also increases activity-dependent Ca^{2+} influx into DGC dendrites, thus facilitating spike-timing–dependent plasticity in human brain.

These results demonstrate that most distal DGC dendrites, like those of many other neurons, are tuned to respond in a nonlinear fashion to activity in the high-frequency gamma range. The downstream effect of this dendritic signal will depend on the complex interplay of dendritic voltage-dependent and receptor-mediated channels. Our results are consistent with the concept that dopaminergic afferents from the VTA can facilitate long-term synaptic plasticity (45), a proxy for hippocampal memory formation (46, 47). We have shown that, during bursting behavior, DGC dendrites can support frequency-dependent activity that can be altered by endogenous neuromodulators, such as dopamine and NPY. Enhancement of dendritic excitability by D1R may result from the reduction of 4-AP–sensitive K^+ channel activity, enhancement of distal dendritic VDCC activity, or both. Irrespective, this increase in activity-dependent dendritic Ca^{2+} influx can facilitate plasticity when there is concurrent input from the MPP. Human DGCs and their inputs exhibit the same mechanism. It is thus likely that during exploration, when place cells fire a burst of APs for a labile representation, a concurrent novelty signal provided by VTA dopamine inputs can initiate plasticity and form a reward-based contextual memory (5–7). This mechanism would also apply during CPP for a drug reward, such as cocaine (5, 6) or nicotine (7) that require dopamine release in the DG. The negative actions of NPY from local neurons downstream of the DGCs could then provide a temporal limit to this process. Finally, given the cAMP dependence of

this mechanism, other chemical messengers whose receptors elevate cAMP may also mediate similar synaptic plasticity.

Materials and Methods

Slice Preparation. Rat experiments were performed in hippocampal slices from 3- to 5-wk-old male (or female where indicated) rats as described previously (48). Rats were decapitated and the brains were removed and placed into an ice-cold (0–4 °C) slicing solution (*SI Materials and Methods*). Transverse slices (300 μM thick; 48) were cut with a vibrating slicer and placed in a 32–34 °C ACSF (*SI Materials and Methods*). Human DG slices were prepared from biopsies obtained during surgical resection from 10 female patients (35–62 y old) and one male patient (36 y old) with medically intractable temporal lobe epilepsy, under a protocol approved by the Health Research Ethics Board of the University of Alberta and Capital Health Authority.

Electrophysiology and Calcium Imaging. Whole-cell patch clamp recordings in DGCs were obtained using glass pipettes (4–6 MΩ) filled with an intracellular solution (*SI Materials and Methods*). In some experiments DGCs were filled with OGB-1 (Invitrogen) and/or 0.001–0.01 Alexa 594 via the whole-cell pipette. See *SI Materials and Methods* for stimulation protocols.

Drugs. All drugs and peptides were dissolved in ACSF and perfused on slices at a flow rate of 2.5–3.5 mL/min unless otherwise noted (*SI Materials and Methods*).

Theta-Burst Pairing Protocol. The theta-burst pairing protocol consisted of the pairing of a medial perforant path EPSP with an action potential (EPSP-action potential; 5-ms interval). A series of 10 trials each consisting of five EPSP- AP pairs at 100 Hz was repeated eight times at theta frequency (5 Hz). Stimulus-intensity response curves for EPSP amplitude were established before TBP, and stimuli evoking a 50% maximum EPSP were used for the remainder of the experiment. EPSPs were recorded as an average of three sweeps (5-s interstimulus interval) once every minute. All DGCs were in the inner or middle GCL.

ACKNOWLEDGMENTS. This work was supported by Canadian Institutes for Health Research (CIHR) Grant MT10520 and CIHR Team on the Neurobiology of Obesity Grant OTG 88592 (to W.F.C.). The University of Alberta Hospitals Foundation provided generous equipment support for this project. We are grateful to Professor Annette Beck-Sickinger (Leipzig, Germany) for the generous gift of the NPY receptor-selective agonists, to Dr. Donald J. Marsh (Merck Research Laboratories) for the generous gift of correolide, and to Dr. John McKean (University of Alberta, Edmonton, AB, Canada) for additional biopsy material. T.J.H. was supported in part by a bursary from the Centre for Neuroscience, University of Alberta. W.F.C. is a medical scientist of the Alberta Heritage Foundation for Medical Research.

1. Jung MW, McNaughton BL (1993) Spatial selectivity of unit activity in the hippocampal granular layer. *Hippocampus* 3:165–182.
2. Smith DM, Mizumori SJ (2006) Hippocampal place cells, context, and episodic memory. *Hippocampus* 16:716–729.
3. Leutgeb JK, Leutgeb S, Moser MB, Moser EI (2007) Pattern separation in the dentate gyrus and CA3 of the hippocampus. *Science* 315:961–966.
4. Lisman JE, Grace AA (2005) The hippocampal-VTA loop: Controlling the entry of information into long-term memory. *Neuron* 46:703–713.
5. Zweifel LS, Argilli E, Bonci A, Palmiter RD (2008) Role of NMDA receptors in dopamine neurons for plasticity and addictive behaviors. *Neuron* 59:486–496.
6. Zweifel LS, et al. (2009) Disruption of NMDAR-dependent burst firing by dopamine neurons provides selective assessment of phasic dopamine-dependent behavior. *Proc Natl Acad Sci USA* 106:7281–7288.
7. Tang J, Dani JA (2009) Dopamine enables in vivo synaptic plasticity associated with the addictive drug nicotine. *Neuron* 63:673–682.
8. Ferbinteanu J, Holsinger RM, McDonald RJ (1999) Lesions of the medial or lateral perforant path have different effects on hippocampal contributions to place learning and on fear conditioning to context. *Behav Brain Res* 101:65–84.
9. Mansour A, et al. (1992) A comparison of D1 receptor binding and mRNA in rat brain using receptor autoradiographic and in situ hybridization techniques. *Neuroscience* 46:959–971.
10. Kampa BM, Letzkus JJ, Stuart GJ (2007) Dendritic mechanisms controlling spike-timing-dependent synaptic plasticity. *Trends Neurosci* 30:456–463.
11. Kampa BM, Letzkus JJ, Stuart GJ (2006) Requirement of dendritic calcium spikes for induction of spike-timing-dependent synaptic plasticity. *J Physiol* 574:283–290.
12. Larkum ME, Kaiser KM, Sakmann B (1999) Calcium electrogenesis in distal apical dendrites of layer 5 pyramidal cells at a critical frequency of back-propagating action potentials. *Proc Natl Acad Sci USA* 96:14600–14604.
13. Hoffman DA, Johnston D (1999) Neuromodulation of dendritic action potentials. *J Neurophysiol* 81:408–411.
14. Verney C, et al. (1985) Morphological evidence for a dopaminergic terminal field in the hippocampal formation of young and adult rat. *Neuroscience* 14:1039–1052.
15. Klapstein GJ, Colmers WF (1993) On the sites of presynaptic inhibition by neuropeptide Y in rat hippocampus in vitro. *Hippocampus* 3:103–111.
16. McQuiston AR, Petrozzino JJ, Connor JA, Colmers WF (1996) Neuropeptide Y1 receptors inhibit N-type calcium currents and reduce transient calcium increases in rat dentate granule cells. *J Neurosci* 16:1422–1429.
17. Kopp J, et al. (2002) Expression of the neuropeptide Y Y1 receptor in the CNS of rat and of wild-type and Y1 receptor knock-out mice. Focus on immunohistochemical localization. *Neuroscience* 111:443–532.
18. Sperk G, Hamilton T, Colmers WF (2007) Neuropeptide Y in the dentate gyrus. *Prog Brain Res* 163:285–297.
19. Pérez-Garci E, Gassmann M, Bettler B, Larkum ME (2006) The GABAB1b isoform mediates long-lasting inhibition of dendritic Ca2+ spikes in layer 5 somatosensory pyramidal neurons. *Neuron* 50:603–616.
20. Staley KJ, Mody I (1992) Shunting of excitatory input to dentate gyrus granule cells by a depolarizing GABAA receptor-mediated postsynaptic conductance. *J Neurophysiol* 68:197–212.
21. Golding NL, Jung HY, Mickus T, Spruston N (1999) Dendritic calcium spike initiation and repolarization are controlled by distinct potassium channel subtypes in CA1 pyramidal neurons. *J Neurosci* 19:8789–8798.
22. Kampa BM, Stuart GJ (2006) Calcium spikes in basal dendrites of layer 5 pyramidal neurons during action potential bursts. *J Neurosci* 26:7424–7432.
23. Andrásfalvy BK, Makara JK, Johnston D, Magee JC (2008) Altered synaptic and non-synaptic properties of CA1 pyramidal neurons in Kv4.2 knockout mice. *J Physiol* 586: 3881–3892.
24. Leranth C, Hajszan T (2007) Extrinsic afferent systems to the dentate gyrus. *Prog Brain Res* 163:63–84.
25. Hoffman DA, Johnston D (1998) Downregulation of transient K+ channels in dendrites of hippocampal CA1 pyramidal neurons by activation of PKA and PKC. *J Neurosci* 18:3521–3528.
26. Martin SJ, Grimwood PD, Morris RG (2000) Synaptic plasticity and memory: An evaluation of the hypothesis. *Annu Rev Neurosci* 23:649–711.
27. Schmidt-Hieber C, Jonas P, Bischofberger J (2004) Enhanced synaptic plasticity in newly generated granule cells of the adult hippocampus. *Nature* 429:184–187.
28. Dietrich D, et al. (1999) Two electrophysiologically distinct types of granule cells in epileptic human hippocampus. *Neuroscience* 90:1197–1206.
29. Heinemann U, et al. (1992) The dentate gyrus as a regulated gate for the propagation of epileptiform activity. *Epilepsy Res Suppl* 7:273–280.
30. Bartesaghi R, Gessi T, Migliore M (1995) Input-output relations in the entorhinal-hippocampal-entorhinal loop: Entorhinal cortex and dentate gyrus. *Hippocampus* 5: 440–451.
31. Stanton PK, Sarvey JM (1987) Norepinephrine regulates long-term potentiation of both the population spike and dendritic EPSP in hippocampal dentate gyrus. *Brain Res Bull* 18:115–119.
32. Sanberg CD, Jones FL, Do VH, Dieguez D, Jr, Derrick BE (2006) 5-HT1a receptor antagonists block perforant path-dentate LTP induced in novel, but not familiar, environments. *Learn Mem* 13:52–62.
33. Sjöström PJ, Rancz EA, Roth A, Häusser M (2008) Dendritic excitability and synaptic plasticity. *Physiol Rev* 88:769–840.
34. Acsády L, Kamondi A, Sík A, Freund T, Buzsáki G (1998) GABAergic cells are the major postsynaptic targets of mossy fibers in the rat hippocampus. *J Neurosci* 18:3386–3403.
35. Davis CD, Jones FL, Derrick BE (2004) Novel environments enhance the induction and maintenance of long-term potentiation in the dentate gyrus. *J Neurosci* 24: 6497–6506.
36. Sierra-Mercado D, Dieguez D, Jr, Barea-Rodriguez EJ (2008) Brief novelty exposure facilitates dentate gyrus LTP in aged rats. *Hippocampus* 18:835–843.
37. Bragin A, et al. (1995) Gamma (40-100 Hz) oscillation in the hippocampus of the behaving rat. *J Neurosci* 15:47–60.
38. Buzsáki G (1989) Two-stage model of memory trace formation: A role for "noisy" brain states. *Neuroscience* 31:551–570.
39. Csicsvari J, Jamieson B, Wise KD, Buzsáki G (2003) Mechanisms of gamma oscillations in the hippocampus of the behaving rat. *Neuron* 37:311–322.
40. Gasbarri A, Packard MG, Campana E, Pacitti C (1994) Anterograde and retrograde tracing of projections from the ventral tegmental area to the hippocampal formation in the rat. *Brain Res Bull* 33:445–452.
41. Huang YY, Kandel ER (1995) D1/D5 receptor agonists induce a protein synthesis-dependent late potentiation in the CA1 region of the hippocampus. *Proc Natl Acad Sci USA* 92:2446–2450.
42. Li S, Cullen WK, Anwyl R, Rowan MJ (2003) Dopamine-dependent facilitation of LTP induction in hippocampal CA1 by exposure to spatial novelty. *Nat Neurosci* 6:526–531.
43. Chen L, Bohanick JD, Nishihara M, Seamans JK, Yang CR (2007) Dopamine D1/5 receptor-mediated long-term potentiation of intrinsic excitability in rat prefrontal cortical neurons: Ca2+-dependent intracellular signaling. *J Neurophysiol* 97: 2448–2464.
44. Beck H, Goussakov IV, Lie A, Helmstaedter C, Elger CE (2000) Synaptic plasticity in the human dentate gyrus. *J Neurosci* 20:7080–7086.
45. Tran AH, et al. (2008) Dopamine D1 receptor modulates hippocampal representation plasticity to spatial novelty. *J Neurosci* 28:13390–13400.
46. Morris RG (2003) Long-term potentiation and memory. *Philos Trans R Soc Lond B Biol Sci* 358:643–647.
47. Whitlock JR, Heynen AJ, Shuler MG, Bear MF (2006) Learning induces long-term potentiation in the hippocampus. *Science* 313:1093–1097.
48. El Bahh B, et al. (2005) The anti-epileptic actions of neuropeptide Y in the hippocampus are mediated by Y and not Y receptors. *Eur J Neurosci* 22:1417–1430.